Diagn Interv Radiol 2019; 25: 14–20

ABDOMINAL IMAGING

ORIGINAL ARTICLE

Focal hypersteatosis: a pseudolesion in patients with liver steatosis

Nurgül Orhan Metin
Ali Devrim Karaosmanoğlu
Yavuz Metin
Muşturay Karçaaltıncaba

PURPOSE
We aimed to describe ultrasonography (US), computed tomography (CT), and magnetic resonance imaging (MRI) findings of focal hypersteatosis (FHS).

METHODS
We retrospectively reviewed our database for patients with hypersteatosis. Over a 5-year period (February 2005 to September 2010) a total of 17 321 patients underwent abdominal CT scan and 28 patients were determined to have FHS. All patients had US, CT, and MRI studies. Size, area, and density measurements were performed on CT images. Fat signal percentage (FSP) was measured on T1-weighted in- and out-of-phase gradient-echo images. FHS was defined based on MRI findings, as an area of greater signal drop on out-of phase images compared with the rest of the fatty liver.

RESULTS
The period prevelance of focal hypersteatosis was measured as 0.16% over the 5-year period. Cancer was the most common diagnosis (22 of 28 patients, 78.5%), with the breast (32.1%) and colorectal (25%) cancers predominating. FHS was seen in segment 4 (n=26, 92.8%), segment 8 (n=1, 3.6%), and segment 3 (n=1, 3.6%). Shape was nodular in 21 patients (75%), while triangular or amorphous in the remaining 7 patients (25%). FHS was hyperechoic and isoechoic in 5 (17.9%) and 23 (82.1%) patients, respectively. FHS was hypodense on CT of all patients relative to fatty liver. On MRI, the FHS was hyperintense on T1-weighted in-phase images in 17 patients (60.7%). Median liver parenchymal FSP was 21.5% (range, 10%–41.4%) and median FSP of hypersteatotic area was 32.5% (range, 19%–45%).

CONCLUSION
Focal hypersteatosis is a pseudolesion that can be observed in patients with liver steatosis. It appears hypodense on CT and mostly isoechoic on US relative to fatty liver. It may mimic metastasis in cancer patients with steatosis, due to nodular shape and atypical location. MRI should be used for correct diagnosis in patients with equivocal findings on CT to avoid biopsy.

Hepatosteatosis is a very common radiologic finding. Global prevalence of nonalcoholic fatty liver disease is 25.24% (1). This finding was also confirmed in autopsy studies with a detection rate of nonalcoholic steatosis in 20%–30% of the cases (2). The detection of this condition is ever increasing due to the refinement in imaging modalities and the increased awareness of this finding by radiologists. The epidemic of obesity and increased insulin resistance, viral hepatitis, metabolic and hereditary disorders, and alcohol abuse should be counted among the most common underlying conditions. Although steatosis is generally a benign finding, subsequent hepatic parenchymal fibrosis and hepatic insufficiency may ensue in a subset of these patients (3). In addition to the aforementioned causes, oncologic patient population is also a growing contributor to this already large patient group. Several chemotherapeutic agents may cause significant steatosis due to their liver toxicity (4–6).

In contrast to diffuse steatosis, focal hepatic hypersteatosis (FHS) is much less known. By definition, FHS refers to a focal area of steatotic liver parenchyma in an already fatty liver (7, 8). These foci may simulate other benign and malignant liver lesions in patients. The correct

From the Liver Imaging Team (M.K. ✉ *musturayk@yahoo.com*), Department of Radiology, Hacettepe University School of Medicine, Ankara, Turkey.

Received 22 December 2017; revision requested 2 February 2018; last revision received 9 June 2018; accepted 3 July 2018.

Published online 17 December 2018.

DOI 10.5152/dir.2018.17519.

You may cite this article as: Orhan Metin N, Karaosmaoğlu AD, Metin Y, Karçaaltıncaba M. Focal hypersteatosis: a pseudolesion in patients with liver steatosis. Diagn Interv Radiol 2019; 25: 14–20.

differentiation is even more important in oncologic patients undergoing chemotherapy, as FHS may simulate liver metastases (3). All cross-sectional imaging modalities including ultrasonography (US), computed tomography (CT), and magnetic resonance imaging (MRI) may be used in the imaging evaluation of these patients.

In this article, we aimed to assess the role of cross-sectional imaging modalities in the diagnosis of FHS with a special emphasis in patients with known malignancies and a history of chemotherapy.

Methods

Patients

This was a retrospective study approved by our institutional review board. Informed consent was obtained from all patients prior to imaging studies. Our institutional database was searched for several keywords including "focal hepatic hypersteatosis", and "focal hypersteatosis". Between February 2005 and September 2010, 17 321 patienst underwent abdominal CT scans, and our keyword searches revealed a total of 28 patients with FSH during this 5-year period. US, CT and MRI studies were available for all 28 patients. These were re-evaluated by two radiologists, both with more than 10 years' experience in abdominal imaging with fellowship training in the field. A final consensus was reached by both radiologists for each case before proceeding to the subsequent case.

Ultrasonography

US studies were performed with several different scanners (Sonoline Ellegra and Sonoline Antares, Siemens Healthcare; Aplio US, Toshiba Healthcare). Wideband convex probes (2–5 Mhz) of these devices were used for liver imaging and the archived images of these studies were used for this study.

Main points

- Focal hypersteatosis (FHS), which refers to more focal fat deposition within an already steatotic liver, is a pseudolesion that can be encountered more often in cancer patients receiving chemotherapy.
- Ultrasonography does not appear to be useful for detecting FHS. CT seems to be more succesful in both detection and characterization, but it may fail to distinguish FHS from other hypodense focal liver lesions.
- T1-weighted in- and out-of-phase MRI images are the most sensitive sequences for detection of FHS; signal drop on out-of-phase images can be used for correct diagnosis especially in cancer patients, to prevent further patient anxiety as well as unnecessary biopsies.

Computed tomography

Different CT scanners were used for liver examinations including 4-MDCT (Somatom Volume Zoom; Siemens Healthcare) and 16-MDCT (Light Speed, General Electric and Somatom Sensation; Siemens Healthcare) scanners. Acquisitions were performed in supine position with 5 mm slice thickness (reconstruction interval, 5 mm), 0.5 s tube rotation time, 1.3–1.5 pitch value, 120 kVp tube voltage, and 100–140 mAs tube current. CT examinations were performed after 110–120 mL nonionic intravenous contrast injection with an injection rate of 3 mL/s at the portal venous phase (70 s after contrast injection). The relevant processing and measurements of the CT images were performed on CT workstations.

We calculated the attenuation difference between the liver and splenic parenchyma, in 28 patients, by two different methods described in the literature (9, 10):

1. Liver parenchymal density / Splenic parenchymal density
2. Liver parenchymal density - Splenic parenchymal density

Magnetic resonance imaging

MRI examinations were performed with three different 1.5T MRI scanners (Siemens Symphony Magnetom, Philips Achieva, and GE Signa HDx) with the 4- and 8-channel phased array body coils. Acquisition parameters included T1-weighted gradient-echo in-phase and out-of-phase sequences (TE in-phase, 4.6 ms or 4.8 ms, out-of-phase, 2.3 ms or 2.4 ms; TR, 94–165 ms; flip angle [FA], 70°–80°; slice thickness, 8 mm; matrix, 256×256), T2-weighted HASTE sequence (TE, 80 ms; TR, 417 ms; FA, 90°; slice thickness, 6 mm; matrix, 256×256), T2-weighted fat-supressed sequence (TE, 80–100 ms; TR, 415–8710 ms; FA, 90°–125°; slice thickness, 6–8 mm; matrix, 512×512). Contrast-enhanced dynamic 3D T1-weighted gradient-echo sequences were also performed after acquisition of the above sequences.

Image analysis of in-phase and out-of-phase MRI sequences

The signal intensity values of FHS foci were obtained by using an average of 0.5 cm^2 region-of-interest (ROI) for liver. As for spleen, 0.5 cm^2 and 1.5 cm^2 ROI circles were used for signal measurement. The ROI was drawn as large as possible for the measurement of liver and spleen parenchyma, excluding the vascular structures. For the signal intensity measurement of FHS in the liver, ROI drawings included the abnormal liver foci completely and excluded the adjacent liver parenchyma. The quantitative measurements were obtained from in- and out-of-phase images of the liver and spleen, using the above approach. Signal intensity indices (SII) were acquired by using the measurement technique defined for adrenal adenoma characterization in the imaging literature (12):

SII (FHS)= [(SI in-phase FHS – SI out-of-phase FHS) / SI in-phase FHS] ×100
SII (liver)= [(SI in-phase liver – SI out-of-phase liver) / SI in-phase liver] ×100
SII (spleen) = [(SI in-phase spleen – SI out-of-phase spleen) / SI in-phase spleen] ×100

Fat signal percentage (FSP) values in the background liver parenchyma and the FHS foci were calculated based on the following formula (12):

FSP = [(liver in-phase/spleen in-phase – liver out-of-phase/spleen out-of-phase)/2(liver in-phase/spleen-in-phase)]×100

Statistical analysis

Statistical analysis was performed using SPSS 15.0 (SPSS Inc.). The descriptive statistics were expressed as mean and standard deviation for continuous variables, median and range for continuous variables with non-normal distribution, frequency and percent for categorical variables. The Pearson corelation test was used for data analysis. A *P* value of less than 0.05 was considered statistically significant.

Figure 1. A 52-year-old female with a history of endometrium sarcoma. Focal hypersteatosis (FHS) is seen as hyperechoic nodular area *(arrow)* in segment 4 adjacent to portal vein on abdominal ultrasonography.

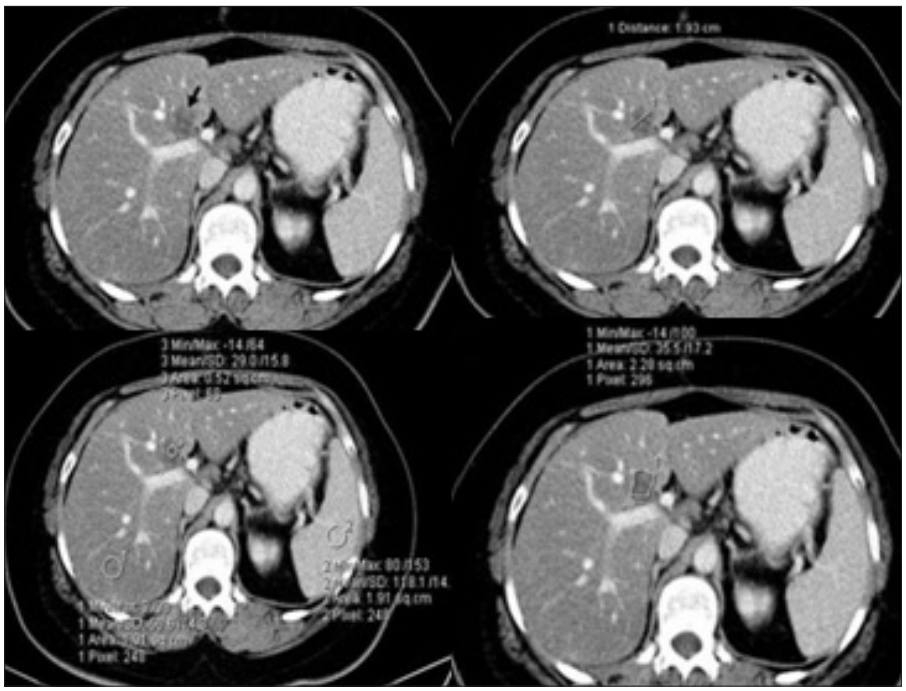

Figure 2. A 44-year-old woman with a history of colon cancer. FHS *(black arrow)* in segment 4 adjacent to porta hepatis on axial contrast-enhanced CT images showing diameter, area, and density measurements.

Table 1. Demographic and clinical characteristics of study population and the chemotherapeutic agents

	n	Chemotherapeutic agents
Patients	28	
Sex (M/F)	6/22	
Age (years), mean±SD	52.3±9.6	
Cancer related	22	
Breast cancer	9	Vinorelbine, docetaxel, clodronate, ietrozole, trastuzumab, capecitabine paclitaxel, dexamethasone sodium phosphate, gemcitabine, cisplatin
Colorectal cancer	7	5-FU, leucovorin oxaliplatin, cisplatin, docetaxel, bevacizumab, irinotecan
Gastric cancer	2	5-FU, leucovorin, cisplatin, docetaxel
Other malignancies	5	Methotrexate, cytarabine, ifosfamide, mesna, etoposide
Noncancer related	6	

M, male; F, female; FU, fluorouracil.

Results

A total of 28 patients were determined to have FHS, making the period prevelance of FHS 0.16% over a 5-year period. Six of these patients had no history of malignancy and the studies were performed for non-cancer-related reasons (elevated liver function tests, acute mesenteric ischemia, umblical hernia, acute pancreatitis, hepatosteatosis, and vasculitis). None of the patients had a history or laboratory findings suggestive of any viral or congenital metabolic disorders affecting the liver. The remaining 22 patients had a history of malignancy (breast cancer (n=9, 32.1%), colon and rectal cancer (n=7, 25%), gastric cancer (n=2, 7.1%), non-Hodgkin lymphoma (n=1), renal cell cancer (n=1), endometrial sarcoma (n=1), neuroendocrine tumor of the pancreas (n=1), and ovarian cancer (n=1) (Table 1). One patient had concurrent breast and colon cancer. There was a history of chemotherapy use within 12 months of the imaging studies in 15 of 22 patients with malignancies, while the remaining 7 patients were all newly diagnosed cases scanned for initial staging and had not received any form of chemotherapy at the time of the imaging examinations (Table 1).

Laboratory parameters of these 28 patients were also evaluated. All laboratory tests were performed within one month of the imaging study. Mild elevation of aspartate aminotransferase (AST, range, 39–56 U/L; reference value, 8–33 U/L) and alanine aminotransferase (ALT) were detected in 6 and 4 patients, respectively (range, 42–71 U/L; reference value, 5–40 U/L). Two patients had no liver function tests (LFT) performed in our hospital. LFT results were within normal limits in the remaining 16 patients at the time of the imaging studies.

US examination was performed in all patients showing diffuse variable increase in the liver parenchyma suggestive of steatosis. FHS was detected in 5 patients (17.9%) and the common sonographic finding in these patients was the detection of a hyperechoic foci (compared with the background liver parenchyma) (Fig.1). In the remaining 23 cases (82.1%), the only sonographic finding was diffusely hypechoic liver parenchyma with no focal abnormality.

CT and MRI studies were available in all 28 patients. The FHS foci were detected on CT examinations and were later confirmed by subsequent MRI.

On CT imaging, the median hepatic and splenic parenchymal density values were found to be 77 HU (range, 3–116 HU), and 104 HU (range, 0–150 HU), respectively. The median value of FHS was 48 HU (range, 16–74 HU).

Based on the formula (Liver parenchymal density / Splenic parenchymal density) the median value was found to be 0.65 (range, 0.05–0.75). By using the formula (Liver parenchymal density – Splenic parenchymal density), the median attenuation difference between the liver and splenic parenchyma was on average -24 HU (range, -21 to -67

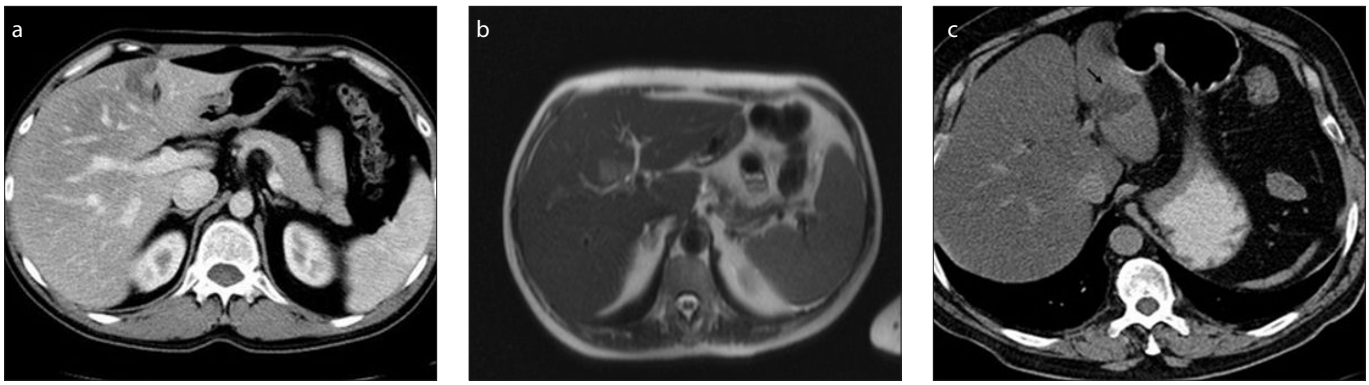

Figure 3. a–c. Distribution of FHS in segment 4 of the liver. Most common location is adjacent to falciform ligament **(a)**, followed by anterior location to the portal vein **(b)**. FHS is also seen in segment 3 **(c)**. Note nodular, amorphous and triangular shape of the pseudolesions.

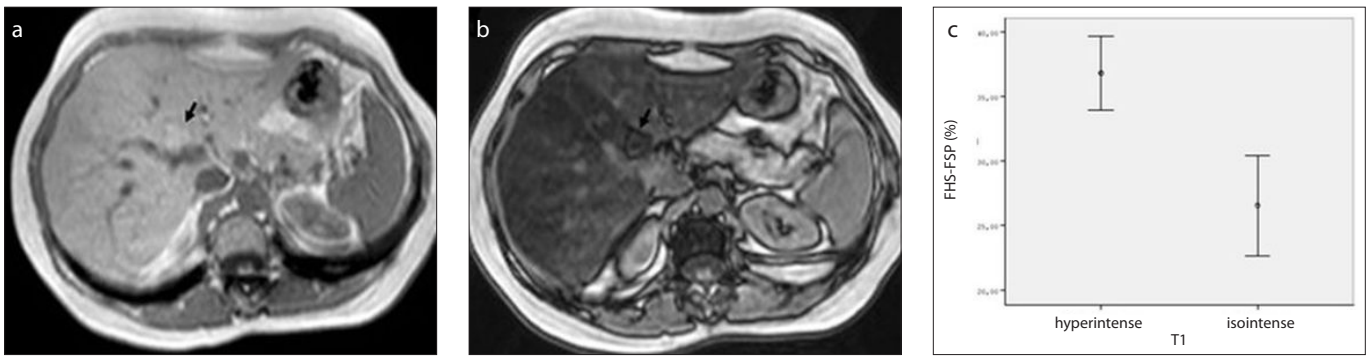

Figure 4. a–c. A 41-year-old female with a history of breast cancer. Axial T1-weighted in-phase gradient-echo image shows sligthly hyperintense FHS in segment 4 adjacent to porta hepatis **(a)**; T1-weighted out-of-phase gradient-echo sequence **(b)** shows signal drop in the same area. Graph **(c)** shows fat signal percentage of patients with hyperintense and isointense FHS on T1-weighted in-phase sequence.

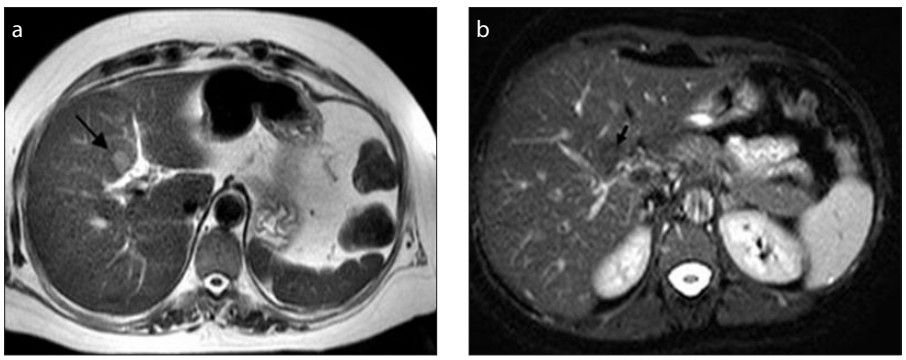

Figure 5. a, b. Axial T2-weighted non-fat-saturated fast spin-echo image **(a)** shows hyperintense FHS area *(arrow)* in a 66-year-old male with a history of steatosis. Axial T2-weighted fat-saturated fast spin-echo image **(b)** shows hypersteatosis as a focal hypointense parenchymal lesion *(arrow)* anterior to portal vein in a 44-year-old female with history of breast cancer.

HU). Both of these values in patients who had CT studies support the presence of steatosis on CT in the portal venous phase at 70 s after contrast injection.

The average size of the detected FHS on both CT and MRI studies was 1.8 cm^2 (range, 0.5–6.0 cm^2) with an average diameter of 1.6 cm (range, 0.8–2.5 cm) (Fig. 2).

The most common location of FHS was segment 4 (n=26, 92.8%); in the remaining 2 patients FSH foci were located in segment 8 (n=1, 3.5%) and segment 3 (n=1, 3.5%) (Fig. 3). The FHS foci detected in segment 4 were located next to the falciform ligament in 17 patients (60.7%), anterior to the portal vein in 7 patients (25%); different locations in segment 4 were detected in 2 patients (7.1%). The shape of the FHS foci was nodular in 21 patients (75%), triangular or amorphous in the remaining 7 patients.

On T1-weighted in- and out-of-phase images, the median liver parenchymal FSP was 21.5% (range, 10%–41.4%), while the median FSP of the hypersteatotic area was found to be 32.5% (range, 19%–45%) (Table 2).

On in-phase T1-weighted images, FHS foci were found to be hyperintense compared with the adjacent liver parenchyma in 17 patients (60.7%) (Fig. 4), while isointense and not discernible in the remaining cases (39.3%). In these patients, the FSP values were found to be higher than the adjacent liver parenchyma.

In the retrospective evaluation of non-fat-suppressed T2-weighted images, the FHS foci were hyperintense compared with adjacent liver parenchyma in 18 patients (64.3%) (Fig. 5a). In the remaining 10 cases (35.7%), these foci could not be detected, as they were isointense.

On fat-supressed T2-weighted images, the FHS foci could not be detected as a seperate abnormal lesion in any of the patients except for one, in whom the FHS was detected as a focal hypointense parenchymal area (Fig. 5b).

Follow-up imaging studies were available in 14 of 28 patients (between 6 and 24 months). The FHS foci were stable with no interval change in size or configuration in 8

Table 2. Imaging appearances of fat-saturated focal hypersteatosis on different imaging modalities and FSP measurements

Modality	Patient number	FSP(%)
US		
Isoechoic	5	37.6
Hyperechoic	23	31.8
CT		
hypodense	28	32.6
T1 in-phase		
Isointense	11	26
Hyperintense	17	36.8
T2-HASTE		
Isointense	10	27.1
Hyperintense	18	36.5
T2-FS		
Isointense	16	32.6
Hypointense	1	43

FSP, fat signal percentage; US, ultrasonography; CT, computed tomography; T2, T2-weighted; HASTE, half-Fourier acquisition single-shot turbo spin-echo; FS, fat-saturated.

patients (57.1%), while they completely disappeared in 4 cases (28.6%). In the remaining 2 cases (14.3%), the lesions appeared to be smaller and were hardly discernible compared with adjacent liver parenchyma.

Discussion

Hepatic steatosis and focal fat deposition are well-known clinical entities. In addition to patients with insulin resistance, obesity, alcohol abuse, and several hereditary/metabolic diseases, history of chemotherapy use in cancer patients is also an important contributing factor to this already large pool of patients. Liver steatosis has been reported to occur in 47% of patients with known colorectal cancer, who received systemic chemotherapy (4). This chemotherapy effect is more pronounced in patients who received folinic acid, floxuridine, and 5-fluorouracil (5-FU) as a part of their regimen (13–15). As all of the above agents were commonly used in our patients' chemotherapy regimens, we also think that they significantly contributed to the findings in our patient cohort. Overall, 25% of the subjects had a history of colorectal cancer in our group, and they all received systemic 5-FU and floxuridine as part of their treatment. Tamoxifen, a medication widely used in the treatment of breast cancer, was also implicated as a causative agent for hepatic steatosis. Tamoxifen was reported to stimulate increased fat deposition within the visceral adipose tissue, as well as the liver (5). A strong relationship between breast cancer and development of fatty liver, treated with chemotherapy regimens with or without tamoxifen, was also reported (6). We also detected a similar relationship in our patient cohort, in which 9 patients (32.1%) had a diagnosis of breast cancer.

Focal fat deposition is a relatively common clinical situation in patients undergoing chemotherapy. The underlying pathophysiology is poorly understood and most of the proposed potentially explanatory theories are mostly speculative. Vascular theory is the most commonly proposed mechanism (16). Vascular supply of the liver other than the hepatic artery and the portal vein is believed to be the underlying mechanism for focal areas of abnormal focal fatty deposition or sparing (17, 18). Aberrant and normal veins that enter the liver independently from the portal vein may have communications with the intrahepatic portal branches; a situation which may give rise to focal perfusional changes and subsequent metabolic alterations within the liver parenchyma (18). Parabiliary venous system drains the pancreatic head which may result in higher concentrations of insulin delivery which, in turn, may induce metabolic changes within the liver parenchyma (17). This argument was supported by focal fatty change beneath the capsule in patients receiving intraperitoneal insulin during peritoneal dialysis (19). The change in the oxygen tension secondary to atypical perfusion should be counted among the potential contributors (20, 21).

The term FHS, which refers to more focal fat deposition within an already steatotic liver, may be inadequate to define this phenomenon. This focal fat deposition, as stated above, may also cause diagnostic confusion in an already steatotic liver parenchyma. In contrast to diffuse or heterogenous parenchmal fatty infiltration of liver, FHS is a relatively less known clinical entity. FHS, as a seperate clinical entity, is relatively newly defined and much less is known about this phenomenon (7, 8).

In our patient cohort, we detected FHS more often in patients receiving chemotherapy. As hepatic steatosis is a common associating phenomenon in patients receiving chemotherapy, this finding is not completely unanticipated.

The relationship between liver function and steatosis was investigated very thoroughly in the medical literature. AST and ALT are the most frequently used laboratory parameters in the investigation of liver function and both were reported as not elevated in the great majority of the patients who received tamoxifen and subsequently developed steatosis (22). We also did not see any abnormalities in the liver function tests of the majority (61.6%) of the FHS cases, which was consistent with the subsequent reports in the literature.

In healthy subjects the fat percentage of the liver parenchyma is less than 5% (10, 23–26). In all our patients, there was abnormally high fat accumulation in the liver: the median fat signal percentage in the liver was 21.5%, consistent with steatosis, while the median fat signal percentage in FHS foci was found to be 32.5%.

The common location of FHS in our cohort was found to be the liver parenchyma adjacent to the falciform ligament (64.2%) followed by the the area anterior to the

main portal vein (28.5%). These two areas are also the most common location of focal fatty deposit, based on the literature findings (10, 21) and, therefore, the diagnosis of FHS might be relatively more straightforward when seen in these locations. Despite this relative easiness of diagnosis in these locations, when FHS is located in atypical liver areas including segment 8 and segment 3, correct diagnosis may be difficult or, even, impossible. It should be be borne in mind that, even when located in these typical locations, metastatic disease should also be considered in the differential diagnosis in patients with known history of malignant disease. Also hypersteatosis can develop on follow-up CT studies as a new lesion, which can be confusing.

Regarding the most reliable imaging modality for diagnosis of FHS, MRI appears to be the reference standard, because it is the only modality that can diagnose hypersteatosis as there is no other lesion demonstrating greater signal drop on T1-weighted out-of-phase images compared with background fatty liver. US could only detect FHS in only 5 of 28 patients in our study, which is not surprising, given the well-known fact that steatosis may significantly limit focal lesion detection in the diffusely steatotic liver parenchyma.

CT images demonstrated FHS foci as hypodense areas in the already steatotic liver parenchyma. Despite the fact that CT appears to be somewhat successful in detecting FHS, it was not helpful in characterizing the lesions as FHS may mimic other benign/malignant focal liver lesions that can appear similarly hypodense on CT.

T1-weighted in- and out-of-phase MRI images emerged as the most sensitive sequences for the detection of FHS. FHS could be detected in all our patients using the out-of-phase gradient-echo sequence. Non-fat saturated T2-weighted images also appear to be helpful for detecting the FHS as moderately hyperintense foci. Although non-fat-supressed T2-weighted images could detect these foci in some patients, it was not possible to characterize them, as metastatic foci also appear as moderately bright on T2-weighted images. Fat-supressed T2-weighted images could not detect FHS in any of our cases which prompts us to suggest that this sequence is useful in neither detection nor characterization of FHS. Although it was not available in our patients, diffusion-weighted imaging can also be helpful in ruling out metastasis in these patients.

Our study also provided some insight regarding the long-term biologic behavior of FHS. Some patients showed complete resolution of these lesions on long-term follow-up, which is an important clue to the dynamic internal metabolic nature of FHS.

From a morphologic standpoint, most of the lesions in our cohort were nodular. This feature is even more confusing for imaging specialists as most liver metastases also appear as round-shaped, nodular/spheric lesions. Although most FHS foci appear as nodular, it should be noted that some lesions appear as poorly defined, irregularly shaped, abnormal parenchymal focal lesions.

Our study has several limitations. As this is a retrospective study, our patient group is heterogeneous, comprising patients who have a history of malignancy and several other patients, who do not have cancer history. Another limitation is the lack of histopathologic diagnosis in all of our patients. However, the typical imaging features on in- and out-of-phase images obviated the need for any invasive procedure, given the 100% specificity of MRI finding of signal drop on T1-weighted out-of-phase images compared with in-phase images. Another limitation is the lack of unenhanced images in our CT group. It is well demonstrated in the literature that unenhanced CT images are more sensitive for detecting steatosis (23, 24), but use of portal venous phase images was reported in the literature (10, 25–28). Moreover steatosis was defined mainly by MRI as the reference standard (29–31) .

In conclusion, FSH is a pseudolesion that can be encountered in patients with steatosis, and MRI is the problem solving method. T1-weighted in- and out-of-phase sequence images should be used for the diagnosis. The common sites of FHS may provide a diagnostic clue; however, a diagnosis of FHS should not be made based on US and CT features as metastatic disease in these locations, albeit rare, may occur. We think that familiarity with the imaging findings of FHS is crucial, especially in cancer patients, to prevent further patient anxiety as well as unnecessary interventions.

Conflict of interest disclosure

The authors declared no conflicts of interest.

References

1. Younossi ZM, Koenig AB, Abdelatif D, Fazel Y, et al. Global epidemiology of nonalcoholic fatty liver disease-Meta-analytic assessment of prevalence, incidence, and outcomes. Hepatology 2016; 64:73–84. [CrossRef]
2. Zhou J, Li YY, Nie YQ, et al. Prevalence of fatty liver disease and its risk factors in the population of South China. World J Gastroenterol 2007; 21:6419–6424. [CrossRef]
3. Karcaaltincaba M, Akhan O. Imaging of hepatic steatosis and fatty sparing. Eur J Radiol 2007; 61:33–43. [CrossRef]
4. Peppercorn PD, Reznek RH, Wilson P, Slevin ML, Gupta RK. Demonstration of hepatic steatosis by computerized tomography in patients receiving 5-fluorouracil-based therapy for advanced colorectal cancer. Br J Cancer 1998; 77:2008–2011. [CrossRef]
5. Nguyen MC, Steward RB, Banerji MA. Relationships between tamoxifen use, liver fat and body fat distribution in women withbreast cancer. Int J Obesity 2001; 25:296–298. [CrossRef]
6. Bilici A, Ozguroglu M, Mihmanli I, Turna H, Adaletli I. A case-control study of non-alcoholic fatty liver disease in breast cancer. Med Oncol 2007; 24:367–371. [CrossRef]
7. Basaran C, Karacaaltıncaba M, Akata D, et al. Fat containing lesions of the liver: Cross sectional imaging findings with emphasis on MRI. AJR Am J Roentgenol 2005; 184:1103–1110. [CrossRef]
8. Idilman IS, Ozdeniz I, Karacaaltıncaba M. Hepatic steatosis: etiology, patterns and quantification,Semin Ultrasound CT MR 2016; 37:501–510. [CrossRef]
9. Kodama Y, Ng CS, Wu TT, et al. Comparison of CT methods for determining the fat content of the liver. AJR Am J Roentgenol 2007; 188:1307–1312. [CrossRef]
10. Zhong L, Chen JJ, Chen J, et al. Nonalcoholic fatty liver disease: Quantitative assessment of liver fat content by computed tomography, magnetic resonance imaging and proton magnetic resonance spectroscopy. J Dig Dis 2009; 10:315–320. [CrossRef]
11. Borra RJH, Salo S, Dean K, et al. Nonalcoholic fatty liver disease: rapid evaluation of liver fat content with ın-phase and out-of-phase MR imaging. Radiology 2009; 250:130–136. [CrossRef]
12. Xiaozhou Ma X, Holalkere NS, Kambadakone RA, Mino-Kenudson M, Hahn PF, Sahani DV. Imaging-based quantification of hepatic fat: methods and clinical applications. Radiographics 2009; 29:1253–1280. [CrossRef]
13. Zorzi D, Laurent A, Pawlik TM, Lauwers GY, Vauthey JN, Abdalla EK. Chemotherapy-associated hepatotoxicity and surgery for colorectal liver metastases. Br J Surg 2007; 94:274–286. [CrossRef]
14. Fernandez FG, Ritter J, Goodwin JW, Linehan DC, Hawkins WG, Strasberg SM. Effect of steatohepatitis associated with irinotecan or oxaliplatin pretreatment on resectability of hepatic colorectal metastases. J Am Coll Surg 2005; 200:845–853. [CrossRef]
15. Masi G, Loupakis F, Pollina L, et al. A long-term outcome of initially unresectable metastatic colorectal cancer patients treated with 5-fluorouracil/leucovorin, oxaliplatin, and irinotecan (FOLFOXIRI) followed by radical surgery of metastases. Ann Surg 2009; 249:420–425. [CrossRef]
16. Patton HM, Lavine JE. Focal fatty liver: more than just a radiographic curiosity? Gastroenterol Hepatol 2007; 3:199–200.
17. Battaglia DM, Wanless IR, Brady AP, et al. Intrahepatic sequestered segment of liver presenting as focal fatty change. Am J Gastroenterol 1995; 90:2238–2239.

18. Yoshimitsu K, Honda H, Kuroiwa T, et al. Unusual hemodynamics andpseudolesions of the noncirrhotic liver at CT. Radiographics 2001; 21:81–96. [CrossRef]
19. Khalili K, Lan FP, Hanbidge AE, et al. Hepatic subcapsular steatosis inresponse to intraperitoneal insulin delivery: CT findings and prevalence. AJR Am J Roentgenol 2003; 180:1601–1604. [CrossRef]
20. Cortez-Pinto H, de Moura MC, Day CP. Nonalcoholic steatohepatitis: from cell biology to clinical practice. J Hepatol 2006; 44:197–208. [CrossRef]
21. Kawamori Y, Matsui O, Takahashi S, et al. Focal hepatic fatty infiltration in the posterior edge of the medial segment associated with aberrant gastric venous drainage: CT, US, and MR findings. J Comput Assist Tomogr 1996; 17:590–595. [CrossRef]
22. Nishino M, Hayakawa K, NakamuraY, Morimoto T, Mukaihara S. Effects of tamoxifen on hepatic fat content and the development of hepatic steatosis in patients with breast cancer: high frequency of ınvolvement and rapid reversal after completion of tamoxifen therapy. AJR Am J Roentgenol 2003; 180:129–134. [CrossRef]
23. Brunt EM. Pathology of fatty liver disease. Mod Pathol 2007; 20:40–48. [CrossRef]
24. Hubscher SG. Histological assessment of non-alcoholic fatty liver disease. Histopathology 2006; 49:450–465. [CrossRef]
25. Jacobs JE, Birnbaum BA, Shapiro MA, et al. Diagnostic criteria for fatty infiltration of the liver on contrast-enhanced helical CT. AJR Am J Roentgenol 1998 171:659–664. [CrossRef]
26. Graffy PM, Pickhardt PJ. Quantification of hepatic and visceral fat by CT and MR imaging: relevance to the obesity epidemic, metabolic syndrome and NAFLD. Br J Radiol 2016; 89:20151024. [CrossRef]
27. Kim DY, Park SH, Lee SS, et al. Contrast-enhanced computed tomography for the diagnosis of fatty liver: prospective study with same-day biopsy used as the reference standard. Eur Radiol 2010; 20:359–366. [CrossRef]
28. Lawrence DA, Oliva IB, Israel GM. Detection of hepatic steatosis on contrast-enhanced CT images: diagnostic accuracy of identification of areas of presumed focal fatty sparing. AJR Am J Roentgenol 2012; 199:44–47. [CrossRef]
29. Özcan HN, Oğuz B, Haliloğlu M, Orhan D, Karçaaltıncaba M. Imaging patterns of fatty liver in pediatric patients. Diagn Interv Radiol 2015; 21:355–360. [CrossRef]
30. Ünal E, Karaosmanoğlu AD, Akata D, Özmen MN, Karçaaltıncaba M. Invisible fat on CT: making it visible by MRI. Diagn Interv Radiol 2016; 22:133–140. [CrossRef]
31. Kramer H, Pickhardt PJ, Kliewer MA, et al. Accuracy of liver fat quantification with advanced CT, MRI, and ultrasound techniques: prospective comparison with MR spectroscopy. AJR Am J Roentgenol 2017; 208:92–100. [CrossRef]